

# RECENT RESULTS FROM THE DISPERSED LIQUID AGENT FIRE SUPPRESSANT SCREEN

Jiann C. Yang, Nikki C. Privé, Michelle K. Donnelly,  
and William L. Grosshandler  
Building and Fire Research Laboratory  
National Institute of Standards and Technology  
Gaithersburg, MD 20899 USA

## INTRODUCTION

Most of the current methods for fire suppression efficiency screening (e.g., cup burners) are designed for evaluating gaseous fire suppression agents. Potential uses of liquid agents as halon replacements have been recently proposed in several applications (e.g., shipboard machinery spaces, engine compartments in armored vehicles). Under the auspices of the US Department of Defense Next Generation Fire Suppression Technology Program (NGP), the National Institute of Standards and Technology (NIST) has been tasked to design, construct, and demonstrate a laboratory-scale apparatus that can perform the screening of liquid agents in well-controlled conditions.

Since the presentation of the first-generation NIST dispersed liquid agent fire suppression screen (DLAFSS) apparatus at the Halon Options Technical Working Conference 1998 [1], several modifications to the apparatus have been made to alleviate clogging in the orifice of the piezo-electric droplet generator when fluids with dissolved solids were used and to accommodate samples available in small quantities. This paper describes the modifications to the apparatus in detail and presents some recent screening results. A test protocol is also proposed for screening liquid agents.

## APPARATUS

The current apparatus consists of a cylindrical (Tsuji-type) opposed-flow burner [2] located in the test section of a vertical wind-tunnel and a droplet generation device mounted in the settling chamber of the tunnel. Figure 1 is a schematic of the test apparatus. The total length of the tunnel from the entrance of the diffuser to the exit of the test section is approximately 1.2 m. The tunnel, except the test section, is made of clear polycarbonate and polymethyl methacrylate for visual observation of droplet transport toward the burner. The test section, with a cross section of 10 by 10 cm, is made of anodized aluminum with three observation windows. Liquid agent droplets are injected from the droplet generator into the flow stream and entrained upward toward the burner for fire suppression effectiveness evaluation. A detailed description of the wind tunnel and the operation of the burner can be found in References 1 and 3.

In the early development stage of the screening apparatus, a piezoelectric droplet generator was used to create liquid droplets ( $< 100 \mu\text{m}$ ) from the controlled breakup of a liquid jet emerging from a sapphire orifice. However, clogging of the orifice constantly plagued the continuous operation of the piezoelectric droplet generator, aggravated by liquids with high loading of dissolved salts. Only distilled and de-ionized water and a few very dilute aqueous solutions have been successfully tested with the droplet generator [4]. A glass nebulizer is currently employed

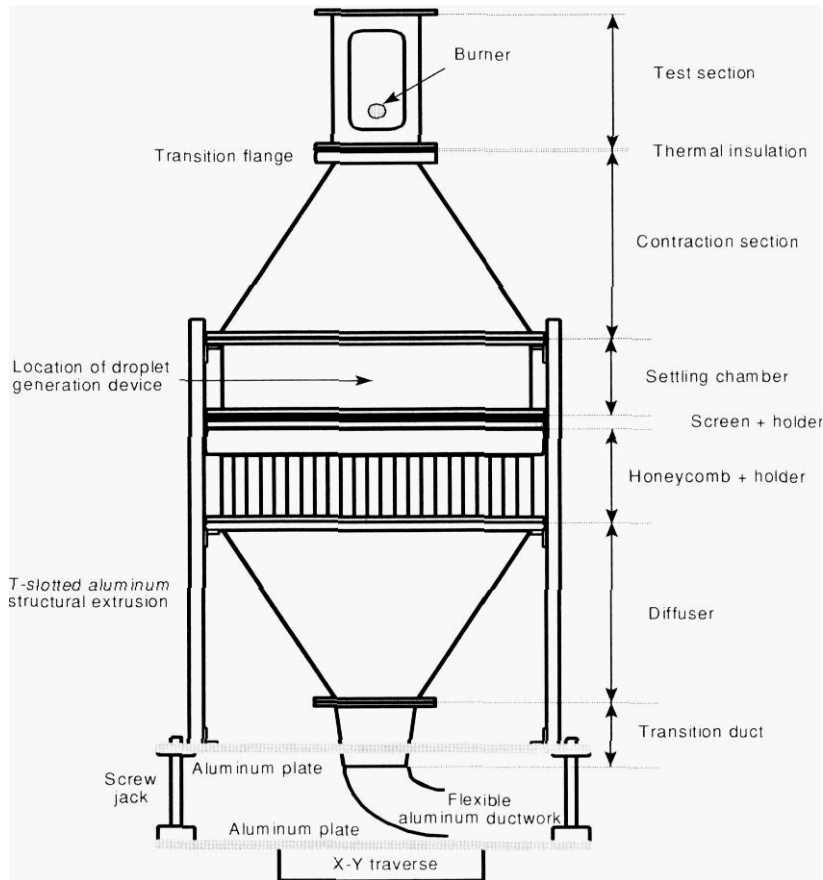


Figure 1. Schematic of the test apparatus.

in the screening apparatus to generate a fine mist of droplets. This type of nebulizer has found applications in inductively coupled plasma (ICP) atomic emission spectroscopy. A schematic of the nebulizer is shown in Figure 2. The selection of an ICP nebulizer is based on its ability to handle a wide range of liquids without clogging and to utilize a small amount of liquid for a test. Aerodynamic break-up of a liquid stream issued from the capillary by high-velocity air causes the formation of a fine mist of droplets. Because of the differences in the droplet formation mechanisms, a relatively large opening ( $\sim 100 \mu\text{m}$ ) of the capillary in the nebulizer, compared to the sapphire orifice ( $\sim 30 \mu\text{m}$ ), can be used. Fluid is fed to the nebulizer by a small syringe pump. Air is supplied to the shell of the nebulizer by a mass-flow controller. The atomizing air flow is set at  $0.25 \text{ L/min}$ , which is the highest flow that can be used without disturbing the flame at the burner. Because of this limit, the atomization efficiency of the nebulizer drops when the liquid delivery rate is increased beyond  $1.3 \text{ ml/min}$ ; that is, larger droplets are generated that may not be entrained upward by the air flow in the tunnel.

The experimental procedure involves the following steps. At a preset liquid delivery rate to the nebulizer, the airflow in the wind tunnel is increased gradually until the transition (blow-off) from an enveloped to a wake flame occurs at the burner; examples of the two types of flame are

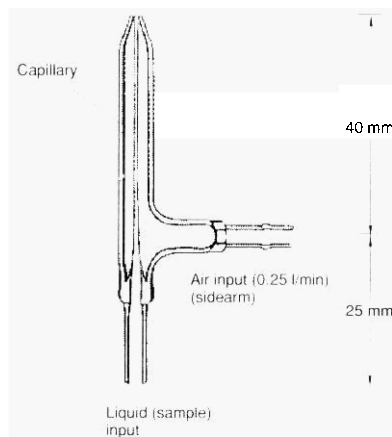


Figure 2. Schematic of the nebulizer.

given in Figure 3. The air velocities at transition are plotted against various liquid delivery rates. The transition velocity is used as a criterion for screening the fire suppression effectiveness of various fire suppressants; the higher the air blow-off velocity, the less effective the fire suppressant.

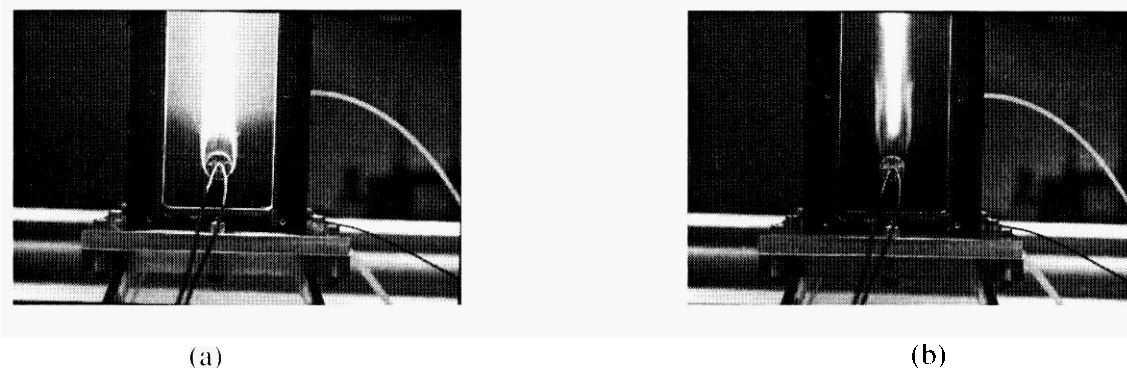


Figure 3. (a) An enveloped flame and (b) a wake flame.

## RESULTS AND DISCUSSION

An Aerometrics two-component Phase Doppler Particle Analyzer (PDPA) with a Doppler Signal Analyzer (DSA) was used to characterize the nebulizer by measuring droplet size and velocity distributions. The measurements were made at several positions near the droplet generation device and near the burner to assess the uniformity of the small droplet spray.

---

Certain commercial products are identified in this paper to specify the equipment used adequately. Such identification does not imply recommendation by NIST, nor does it imply that this equipment is the best available for the purpose.

PDPA measurements of the nebulizer spray were taken on the centerline, 2 cm downstream of the nebulizer exit. Air was supplied to the nebulizer at 0.25 L/min, and deionized water was used as the measurement liquid. The liquid flow rate was varied from 0.3 ml/min to 1.2 ml/min. Unlike the piezoelectric droplet generator, the nebulizer creates droplets with a range of diameters, as evident in the PDPA measurements [3].

PDPA measurements were also taken on the centerline at the burner location. Since the experiment protocol requires the blower air speed to increase until blow-off occurs, it is necessary to determine whether such an increase could result in secondary disintegration of the droplets due to increasing aerodynamic forces on the droplets. Droplet size measurements were taken at blower air speeds of 111 cm/sec and 179 cm/sec. The change in blower air speed within the range for the experiments was found to have a negligible effect on the diameter of the droplets that reached the burner. The Sauter mean diameter (based on the ratio of droplet volume to droplet surface area) is in the range of 25  $\mu\text{m}$  to 35  $\mu\text{m}$  for all air velocities and water application rates. There is a slight tendency for the droplet diameter to increase with liquid delivery rate.

Droplet size measurements were also performed by varying the nebulizer to different off-center locations in the settling chamber to account for possible misalignments, and this was found to have no effect on the droplet size near the burner.

Since the atomizing characteristics of the nebulizer depend on the physical properties of the fluids [5], different droplet size distributions may result when different test fluids are used; this could complicate the interpretation of the screening results by introducing the additional effect of droplet diameter. A series of measurements was performed using the PDPA to determine the dependence of droplet size on the physical properties of the test fluids. Several surrogate fluids (water, 30% and 45% [by mass] potassium lactate, and 1000 mg/l and 2000 mg/l sodium dodecyl sulfate [SDS]) were used to simulate variations in densities, viscosities, and surface tensions. Table 1 lists some of their physical properties. Figure 4 shows the PDPA measurement results on the centerline, 2 cm downstream of the nebulizer exit for liquid flow rates between 0.3 ml/min and 0.9 ml/min. In all cases, the Sauter mean diameters only vary between 20  $\mu\text{m}$  and 30  $\mu\text{m}$ . Differences between diameters of the various liquids are considered to be small, given an estimated uncertainty of 5  $\mu\text{m}$  in the droplet size measurements.

TABLE 1. PHYSICAL PROPERTIES OF SURROGATE FLUIDS.

Fluid	Density ( $\text{g/cm}^3$ ) $\nabla$ 0.01	Viscosity* ( $\text{g/s cm}$ ) $\nabla$ 0.001	Surface tension <sup>†</sup> ( $\text{dyne/cm}$ ) $\nabla$ 1
Distilled water	1.00	0.010	72
30% potassium lactate	1.15	0.025	66
45% potassium lactate	1.23	<b>0.038</b>	<b>68</b>
1000 mg/l SDS	0.98	0.0095	52
2000 mg/l SDS	0.96	0.0093	38

\* Measured using a Cannon<sup>1</sup> Glass Capillary Viscometer

<sup>†</sup> Measured using a DuNouy<sup>®</sup> Tensiometer (Model No. 70535, CSC-Scientific Co., Inc.)

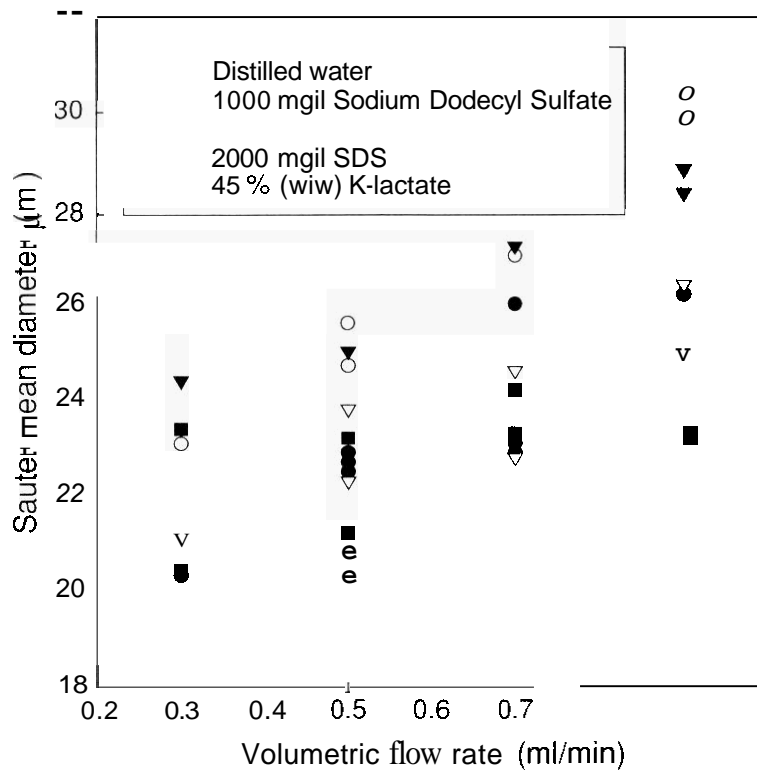


Figure 4. Droplet diameter measurements of various fluids using the PDPA at the centerline location, 2 cm downstream of the nebulizer exit.

Figure 5 shows the various flame stability regions of the burner obtained from the test facility. Each data point on the upper curve was obtained by maintaining a fixed fuel flow and increasing the air flow until blow-off occurred. The regions below and above the curve correspond to the existence of a stable enveloped blue flame and a wake flame, respectively. There is a critical air velocity above which a stable enveloped flame can no longer be established, irrespective of the fuel flow. This critical blow-off velocity depends on fuel type and burner diameter [2]. Each data point on the lower curve was obtained by increasing the fuel ejection rate at a fixed oxidizer flow until a luminous yellow zone appeared. The conditions below this curve represent the existence of a yellow luminous zone. For our proposed *liquid* screening applications, the fuel flow is always fixed at 2 L/min, which corresponds to an ejection velocity of 4.2 cm/sec. The rationale for choosing this value is elucidated in Reference 3.

The above test procedure can be used for rapid screening. A blow-off experiment without agent is first conducted to check the burner performance, followed by a blow-off experiment with a fixed agent application rate. This process is shown schematically as the vertical line in Figure 6. The blow-off velocities are used to provide a *relative* ranking of various liquid agents. Figure 7 shows the screening results using several test fluids. Each data point represents one test. For a given fluid, increasing the liquid application rate decreases the blow-off velocity. As expected, 60% (by mass) potassium lactate is more effective than 30% potassium lactate. Water is the least effective when compared to skim milk, 30% sodium iodide, and 60% potassium acetate. Based on this set of data, the repeatability from run-to-run using the liquid screening apparatus is estimated to be better than 20%.

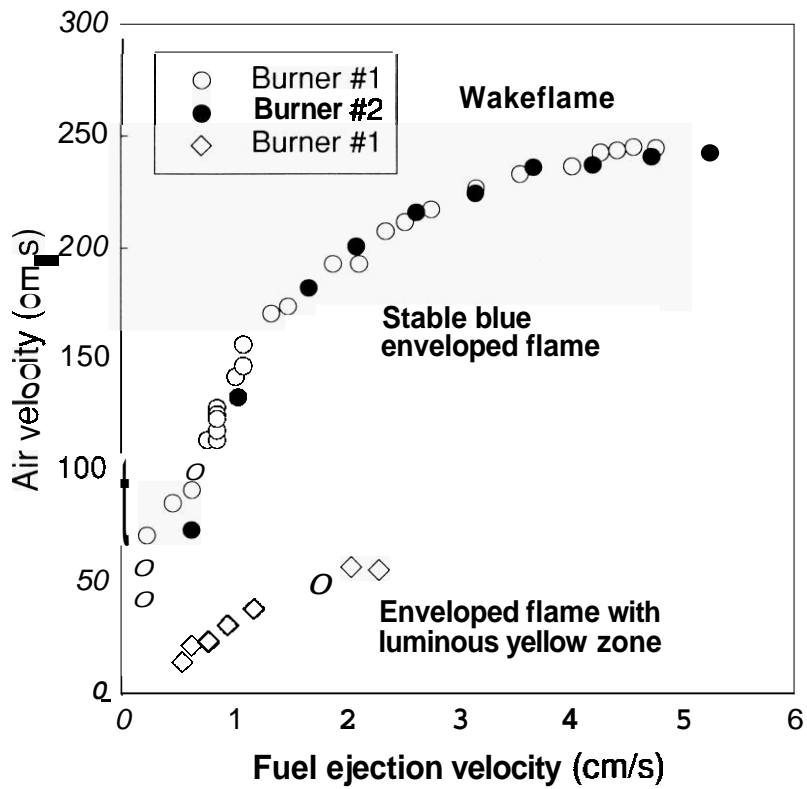


Figure 5. Flame stability (blow-off) curve.

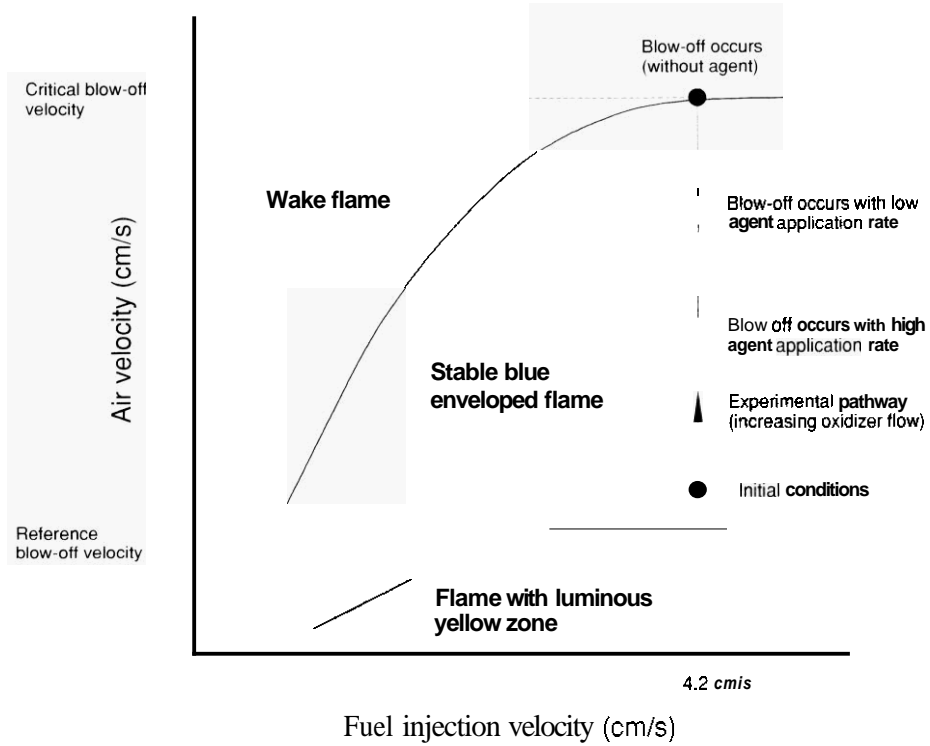


Figure 6. Schematic illustrating the experimental procedure.

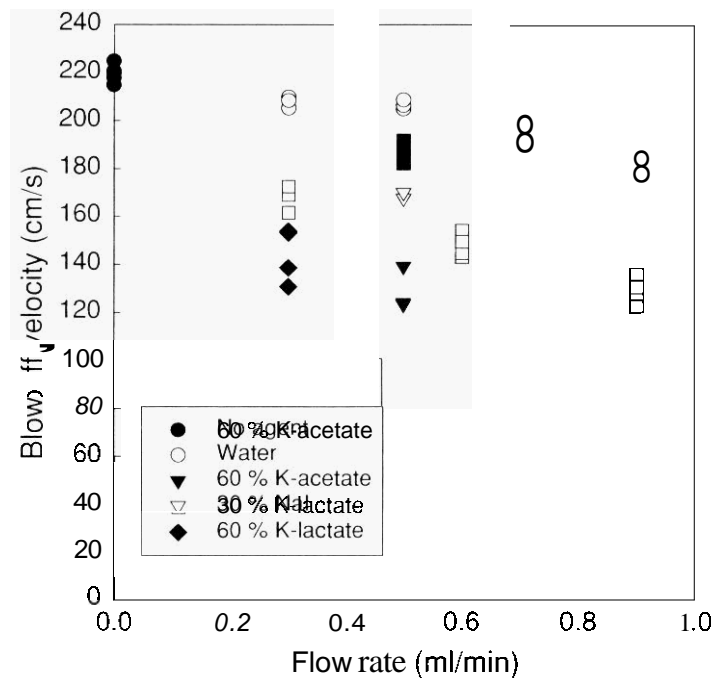


Figure 7. Recent screening results using different types of fluids

Since there are many liquid delivery rates that one can use in the screening procedure, a reference delivery rate is needed to compare and interpret the fire suppression effectiveness of various liquid agents in a consistent and meaningful way. We have developed the following protocol, which is based on the conditions commensurate with the cup-burner results for nitrogen.

The propane cup-burner value for nitrogen is 32% (by mass) [6]. An examination of the results in Reference 3 for a propane flow of 2 L/min (selected to eliminate fuel flow effects and heat transfer to the burner) indicates that the nitrogen mass fraction (at blow-off) equivalent to the cup-burner value corresponds to an air velocity of 30 cm/sec. At this velocity and a propane flow of 2 L/min, a flame cannot be stabilized in the desired blue enveloped flame region (refer to Figures 5 and 6). In addition, the experimental protocol calls for increasing the air velocity (i.e., moving away from 30 cm/sec) until blow-off at a fixed fluid delivery rate. Therefore, in order to compare the results obtained from the cylindrical burner to conditions commensurate with cup-burner results, extrapolation to lower air velocity is required.

Figure 8 demonstrates the proposed extrapolation mechanism. A blow-off air velocity without fluid application is obtained, followed by a blow-off experiment with a fixed fluid application rate. The fluid delivery rate at an air velocity of 30 cm/sec is then deduced by linear extrapolation. Based on our experience, an application rate between 0.6 ml/min and 1 ml/min appears to be appropriate, which is a balance between minimizing the fluid consumption for a test and attaining a blow-off velocity close to the reference blow-off velocity of 30 cm/sec.

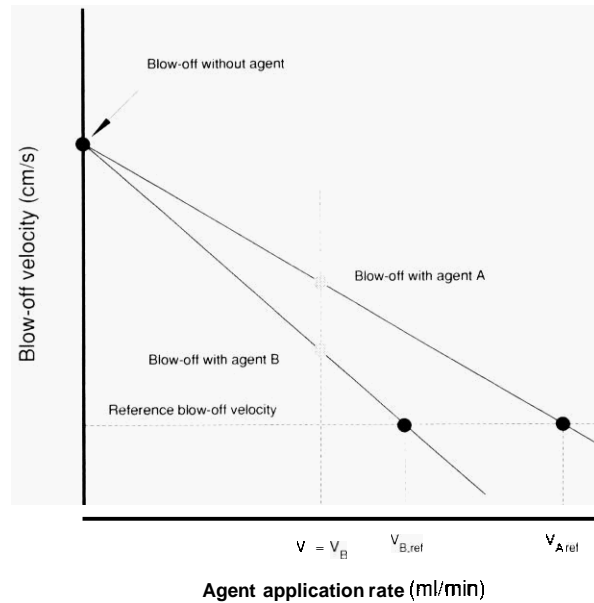


Figure 8. Schematic illustrating the extrapolation of agent application rates at the reference blow-off velocity.

Once the application rate corresponding to the reference blow-off velocity is deduced, the reference mass flow rate of the liquid agent,  $\dot{m}_{agent,ref}$ , can be calculated using the liquid density. The reference mass fraction of the liquid agent in the air stream is then

$$Y_{agent,ref} = \frac{\dot{m}_{agent,ref}}{\dot{m}_{agent,ref} + \dot{m}_{air,ref}} \quad (1)$$

where  $\dot{m}_{air,ref}$  is the mass flow of air, calculated based on the cross-sectional area of the test

section and 30 cm/sec. Note that in writing Equation (1), it is implicitly assumed that the droplets are homogeneously dispersed in the carrier phase (air).

Table 3 summarizes the calculations of the reference agent mass fraction in air using the screening results from Figure 7 and the proposed approach described above. Average values of the blow-off velocities were used in the extrapolation. For cases where blow-off velocities at more than one liquid application rates are available, linear regressions were used to extrapolate the reference blow-off velocities. When data with one application rate were available, simple linear extrapolation was applied to obtain the reference blow-off velocities.

The last column of Table 3 lists the ranking indices relative to water. For example, the 60% K-acetate and K-lactate solutions are considered to be four times more effective than water at the reference blow-off velocity. If the droplets are not homogeneously dispersed across the total cross-sectional area, the calculated agent mass fraction will be underestimated because  $\dot{m}_{air,ref}$  is overestimated. The effective area can be considered as the effective coverage area of the mist in the test section. Depending on the effective coverage area, a difference of a factor of 2 to 3 in the calculated liquid mass fraction can result. By placing a filter paper over the exit of the test

TABLE 3. CALCULATED AGENT MASS FRACTIONS AT REFERENCE BLOW-OFF AIR VELOCITY OF 30 cm/sec.

Agent	$V_{agent, ref}$ (ml/min)	Agent density (g/cm <sup>3</sup> ) @ 20 °C	$\dot{m}_{agent, ref}$ (g/s)	Nominal agent mass %	$\frac{\dot{m}_{water, ref}}{\dot{m}_{agent, ref}}$
Water	4.62	1.00	0.08	2.6	1.0
60% K-acetate	0.99	1.34	0.02	0.8	4.0
30% NaI	1.76	1.29	0.04	1.3	2.0
Skim milk	2.78	1.01	0.05	1.6	1.6
30% K-lactate	1.74	1.15	0.04	1.2	2.0
60% K-lactate	0.71	1.33	0.02	0.6	4.0

section for a short duration with the wind tunnel operating (without the burner) and the nebulizer atomizing water with a dye added, the droplet-impact (color) pattern on the filter paper can be visualized and used as an indicator to determine the mist coverage area in the test section. The color pattern, which is approximately circular, indicates that the mist from the nebulizer completely covers the burner and its vicinity. The mist coverage area was estimated to be ca. 50% of the total cross-sectional area of the test section for all the conditions encountered in our screening tests.

Irrespective of the uncertainty associated with the estimated agent mass concentration, water and the aqueous agents studied here are found to be more effective than CF<sub>3</sub>Br, compared to the propane cup-burner value (17% by mass) for CF<sub>3</sub>Br [6]. The computational study by Lentati and Chelliah [7] also demonstrates that 20- $\mu$ m water droplets are more effective (4.24% vs. 5.9% by mass) in extinguishing an opposed-flow methane diffusion flame than CF<sub>3</sub>Br at an extinction strain rate of  $\approx 176 \text{ sec}^{-1}$ . Although the ratio of our calculated nominal water mass fraction to the cup-burner value for CF<sub>3</sub>Br using propane is smaller, both studies are in qualitative agreement in terms of the suppression effectiveness of water droplets.

Care should be exercised when interpreting the screening results in Table 3, which were obtained using an idealized laboratory flame and a droplet delivery system such that the transport of fine liquid droplets to the flames is not a factor in determining the suppression effectiveness. In the case of real fires, droplet entrainment and transport to the fire can significantly affect the liquid agent mass concentration required to suppress a fire, especially in highly obstructed enclosure fires.

### CONCLUDING REMARKS

The apparatus for screening liquid fire suppressants (DLAFSS) that we have developed has been modified to accommodate fluids with high dissolved-solid loading. The device is robust and easy to operate. An important feature of the apparatus is the requirement of a small amount of fluid to perform a test. The capability of the current device could be potentially extended to screen powder agents by incorporating a (yet-to-be-designed) powder delivery system. The apparatus is currently used to examine aqueous solutions with other additives and potential new liquid agents.

## ACKNOWLEDGMENTS

This research is funded by the Department of Defense Next Generation Fire Suppression Technology Program, funded by the DoD Strategic Environmental Research and Development Program. The authors would like to thank Dr. Marc Rumminger of NIST for reading the manuscript and providing many useful comments.

## REFERENCES

1. Yang, J.C., Donnelly, M.K., Privé, N.C., and Grosshandler, W.L., "An Apparatus for Evaluating Liquid Fire Suppression," *Proceedings*, Halon Options Technical Working Conference, Albuquerque, New Mexico, pp. 471-481, 1998.
2. Tsuji, H. and Yamaoka, I. "The Counterflow Diffusion Flame in the Forward Stagnation Region of a Porous Cylinder," *Eleventh Symposium (International) on Combustion*, The Combustion Institute, Pittsburgh, PA, pp. 979-984, 1967.
3. Yang, J.C., Donnelly, M.K., Privé, N.C., and Grosshandler, W.L.. "Dispersed Liquid Fire Suppression Screen Apparatus," NISTIR-6319, National Institute of Standards and Technology, Gaithersburg, MD (in preparation).
4. Yang, J.C., Donnelly, M.K., Privé, N.C., and Grosshandler, W.L., "Fire Suppression Efficiency Screening Using a Counterflow Cylindrical Burner," *Proceedings of the 5<sup>th</sup> ASME/JSME Joint Thermal Engineering Conference*, San Diego, California, March 1999.
5. Bayvel, L. and Orzechowski, Z., *Liquid Atomization*, Taylor and Francis, Washington, DC, 1993.
6. Grosshandler, W.L., Gann, R.G., and Pitts, W.M., "Evaluation of Alternative In-Flight Fire Suppressants for Full-Scale Testing in Simulated Aircraft Engine Nacelles and Dry Bays," NIST SP861, US Department of Commerce, April 1994.
7. Lentati, A.M. and Chelliah, H.K., "Physical, Thermal, and Chemical Effects of Fine-Water Droplets in Extinguishing Counterflow Diffusion Flames," *Twenty-Seventh Symposium (International) on Combustion*, The Combustion Institute, Pittsburgh, PA, pp. 2839-2846, 1998.